

## Accurate Tool Servo Control for Precision Diamond Turning

Kenneth C. Johnson, March 13, 2019

### Abstract

An order-of-magnitude improvement diamond turning accuracy can be achieved by interferometrically characterizing a workpiece's surface form error, and then applying a shallow trim cut with optical profilometry incorporated in the mechanical servo loop to accurately control and correct the cutting depth.

\*\*\*

Precision Diamond Turning (PDT) is a commonly-used method for fabricating optical components. One example of a state-of-the-art PDT system is the Nanoform 1000 (manufactured by Precitech [1]), which has a 1-meter swing diameter and has a form accuracy specification of 125 nm P-V and surface finish of 1.25 nm Sa. For applications such as EUV lithography and synchrotron X-ray optics the form and finish accuracy can both be of order 0.2 nm [2], which can be achieved by post-polishing a diamond-turned part.

Some EUV/X-ray applications require blazed (sawtooth-profile) reflection gratings, which can be diamond-turned but cannot be post-polished by conventional means to achieve the requisite shape and smoothness requirements. An alternative method, anisotropic etching of silicon, can form geometrically perfect gratings with surfaces defined by the silicon crystal planes, but this method is inapplicable to gratings on curves substrates. [3]

Synchrotron gratings have been made with a mechanical ruling engine by patterning the grating in a gold layer on silicon, and then etching the gold to transfer the pattern into the silicon. The silicon etches much slower than the gold, so the grating's depth dimensions, including its form and finish errors, are scaled down by the etch process. For example, Siewert et al. used this method to reduce an X-ray grating blaze angle from  $6.6^\circ$  to  $0.62^\circ$ , and the surface roughness was reduced from 0.56 nm r.m.s. to 0.12 nm r.m.s. [4] The method could be modified to use other etch chemistries, e.g. with PMMA used as a sacrificial layer instead of gold.

Siewert's method applies to nearly straight-line gratings on nearly flat substrates. In principle, the method could be used for diamond turning of circular gratings, which would be useful for EUV collection mirrors [5]. But the accuracy of diamond turning is not as good as mechanical ruling and may be inadequate even with the error scale reduction of the selective etch process. The grating can be patterned in a substrate that has been machined and polished to a very accurate form specification, but the PDT machine cannot maintain the accuracy during grating formation because the tool positioning system, which relies on stage interferometers, does not provide a direct measure of either the cutting tool's proximity to the workpiece or the depth of cut.

This limitation can be overcome by using accurate surface profilometry to provide feedback to the tool servo system for controlling the depth of cut. This method would be useful

for general-purpose diamond turning of smooth surfaces for optics or other applications in addition to grating manufacture. A conventional mirror or lens would be fabricated by the following steps: (1) Form a curved surface in an optical substrate via conventional diamond turning. (2) Interferometrically measure the surface form error. (3) Apply a PDT trim cut, using an accurate step height gauge to control the depth of cut. (The target cutting depth, as a function of position, is known from the interferometric error map.) (4) Apply a post-polish process to achieve the requisite surface smoothness.

Step 3 is illustrated schematically in Figure 1. In this illustration, the step-height gauge focuses an optical probe beam onto the cut step behind the diamond tool. The diamond tool has a large-radius or straight cutting edge, which is kept tangent to the workpiece surface to form a smooth trim cut. (The lathe's rotational B axis is used to maintain the tangency angle.) The cutting edge terminates at a sharp point to form a distinct cut step, which the height gauge can measure.

Rather than using the height data to directly control the lathe's servo system, it might be simpler and more efficient to use a separate positioning micro-actuator, which is closely coupled to the cutting tool, to make corrective positional adjustments based on the height gauge feedback. A small piezoelectric actuator could provide positional control over a submicron range with better than 0.1-nm resolution. The height gauge and micro-actuator can be integrated in a specialized tool-post accessory, which is used for trim-cut operations. The lathe's control system would not need to use the height sensor feedback information, except perhaps to keep the micro-actuator operating near the middle of its positional range.

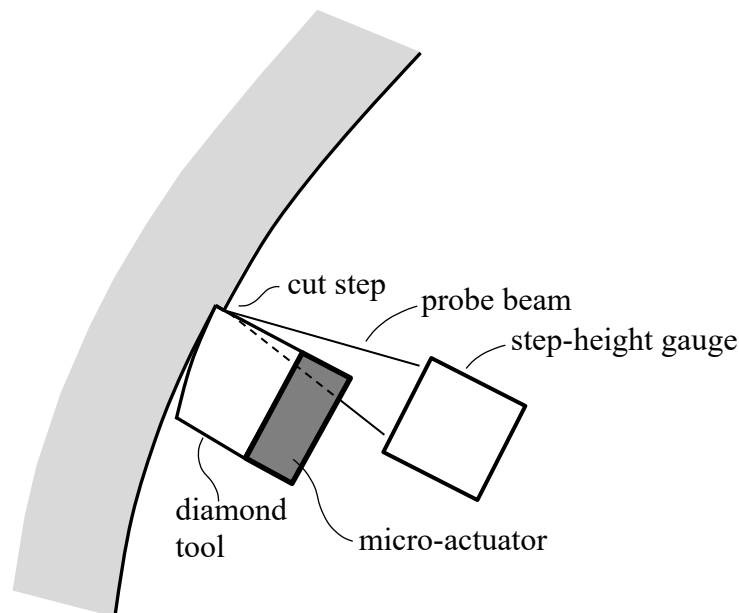


Figure 1

In a variant of the above process, a polishing step is performed before the interferometric data is collected (step 2), and Siewert's method is applied to achieve a smooth trim cut without post polishing. The trim cut would be made in a sacrificial layer such as gold, which would subsequently be removed in a selective etch process. This would eliminate any surface accuracy degradation from post polishing. Also, the process would be applicable to blazed gratings, which cannot be post-polished by conventional means.

The trim cut might need to be done without cutting fluid, which could interfere with the step height measurement. The trim cutting depth would typically be sub-micron, so heat generation would be minimal. If a cutting fluid is required for tool cooling, liquid nitrogen could be used and an air jet could clear out residual fluid.

An optical sensor using single-point optical scattering could be used to measure the step height. The principle of operation is illustrated in Figure 2. A light beam is focused to a diffraction-limited spot straddling the step, which induces a lateral shift in the far-field reflected beam. The sensor mechanism is analogous to two-beam interferometry, in the sense that the far-field diffraction pattern is determined by the optical phase difference between the two parts of the beam on either side of the step. But a closer analogy is the geometric-optics effect of a tilted reflective surface. A sharp step would be below the optical resolution limit, but its optical phase effect would be similar to a tilted surface whose tilt angle is roughly equal to the ratio of the step height to the diffraction-limited beam width. Focusing optics would collect the reflected beam and direct it onto a position-sensing detector, which detects the tilt-induced positional shift. The fractional signal change from the step difference would be expected to be comparable to the height-to-wavelength ratio. For example, with a 250-nm probe wavelength a 1-nm height difference would result in a signal change of order 0.4%.

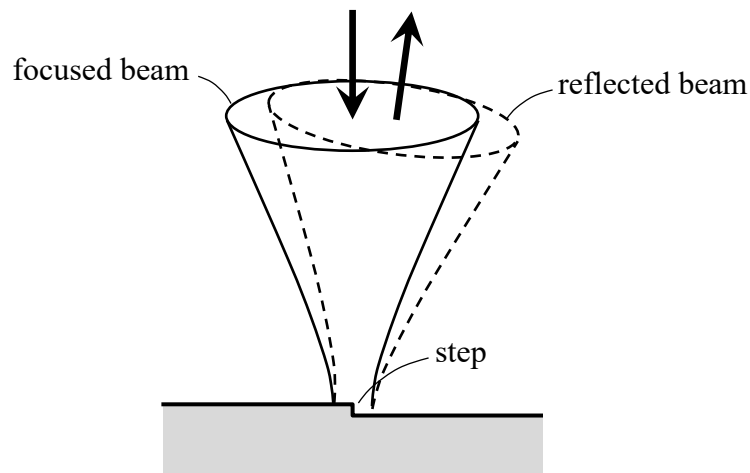


Figure 2

Multiple probe beams are focused onto the workpiece to form a raster image of the surface in the vicinity of the step. Figure 3 shows a face view of the workpiece surface, which is illuminated by a multiple probe beams covering a matrix of focus spots. The matrix rows are slightly angled to the step edge so that the probe beams cover a range of lateral displacement offsets from the step. The multiple probe beams provide information on their lateral alignment

relative to the step, in addition to step height information. Some of the optical probes can also monitor focus alignment via confocal imaging. The spots covering flat areas away from the edge are used for focus control, and also for bias-compensating the depth measurement.

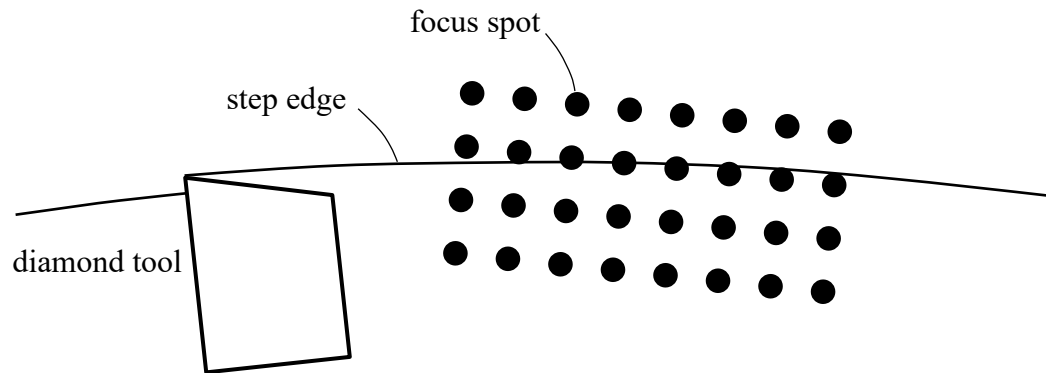


Figure 3

The raster imaging could be useful for manufacturing blazed gratings, as illustrated schematically in Figures 4 and 5. Initially, the grating is cut into an interferometrically-characterized surface, using the height gauge to control the depth of cut (Figure 4). But the lateral positions of the grating steps are at this stage determined by the lathe accuracy. If necessary, the accuracy error can be corrected by performing a second interferometric characterization of the workpiece to determine the grating's phase error. A mapping of the grating steps' lateral positioning errors is determined from the phase map. A second trim cut is performed (Figure 5) to reform the steps with the correction applied, using the previously-cut steps as lateral and depth alignment references. (A positioning micro-actuator with two-axis motion would be required in this mode of operation.)

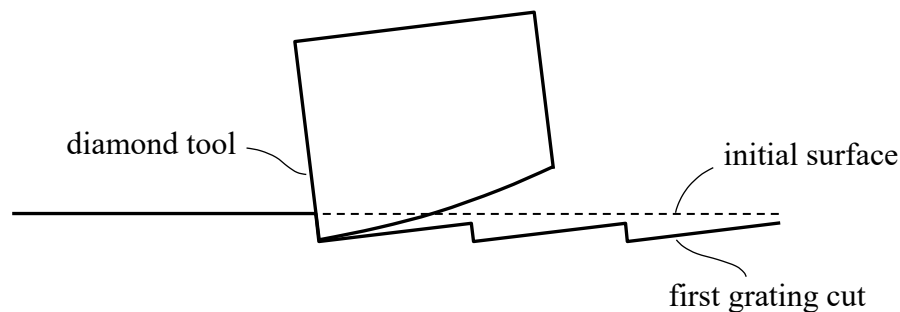


Figure 4

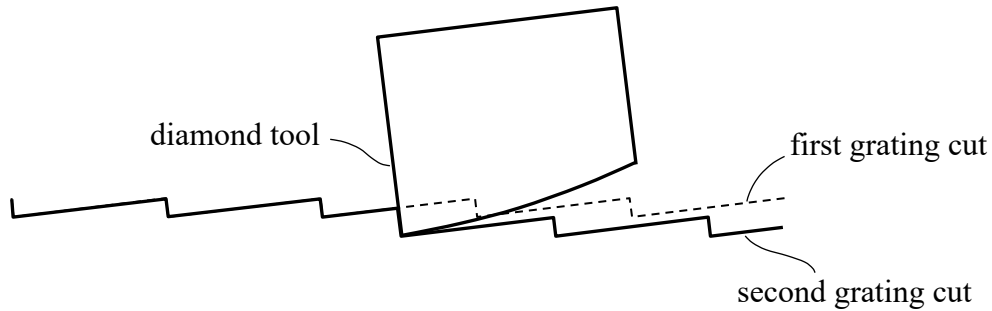


Figure 5

Aside from their application to EUV/X-ray mirrors, blazed gratings would also be useful for visible-light and UV transmission optics [6-9]. For laser optics, the number of design degrees of freedom can be doubled by using phase-Fresnel lens surfaces, and narrow-band achromatization can be achieved with a single glass material. DUV lithography optics could be greatly simplified and could be achromatized to obviate the need for line-narrowed lasers. Improved diamond turning accuracy would also be useful for achromatizing Fresnel-lens solar concentrators.

The height gauge can be implemented as an optical microscope adapted for profilometry, as illustrated schematically in Figure 6. The microscope comprises a number of sensor units, which direct laser illumination through a projection system onto the workpiece surface and collect the reflected radiation returned from the surface. Each unit both generates an illumination beam, which is focused by the projection optics onto a diffraction-limited focus spot on the workpiece, and collects the reflected return radiation as the workpiece is scanned across the focal point array to construct a raster image of the surface.

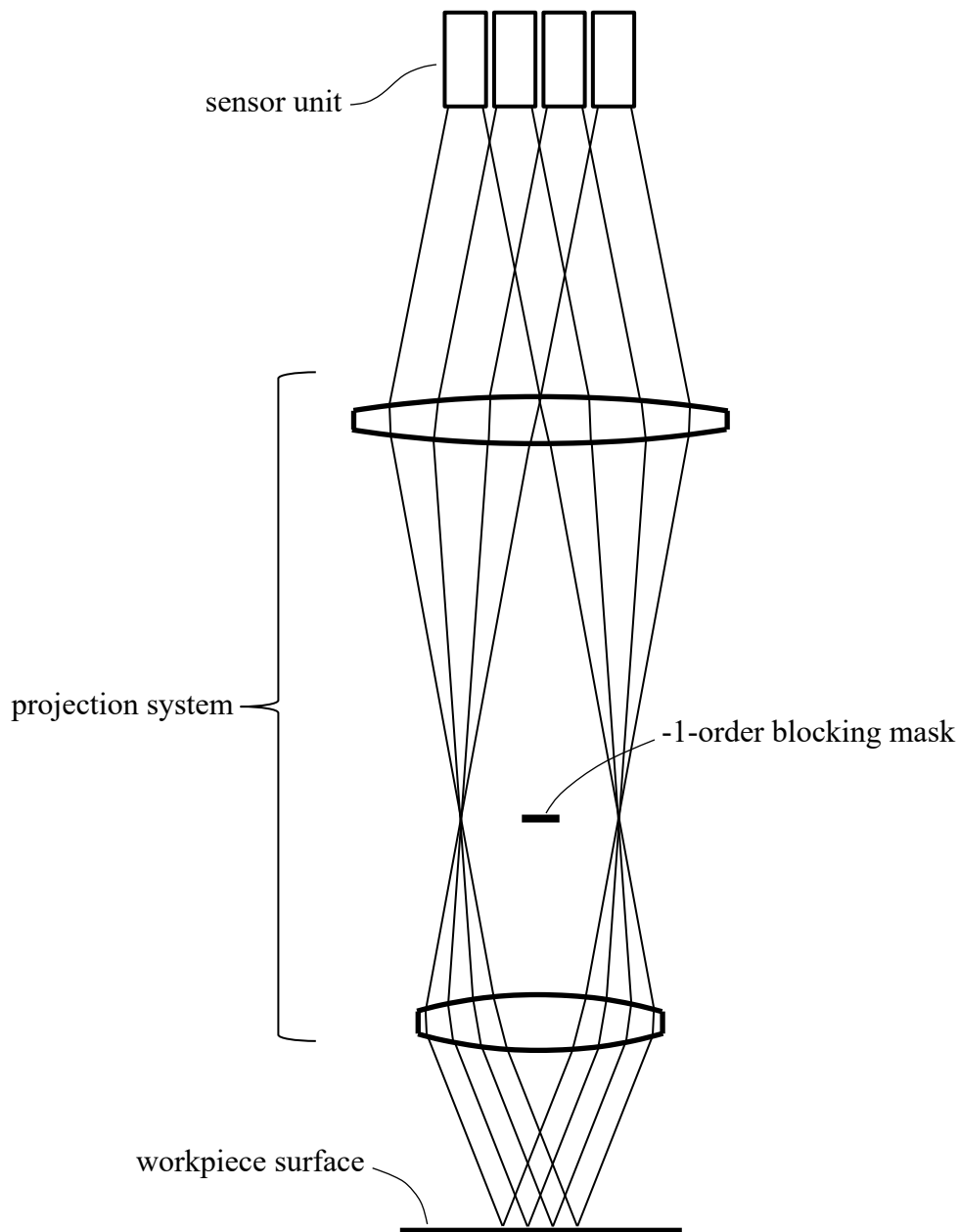


Figure 6

Figures 7 and 8 schematically illustrate the internal structure of a sensor unit, which has both step-height and focus sensing capabilities. Laser radiation is brought into the system by focusing a beam through a pinhole spatial filter at point  $P_0$ . (Alternatively, the illumination can be delivered through an optical fiber terminating at  $P_0$ , although a focused beam would provide more control over the beam quality.) The beam passes through a diffractive, diverging microlens, which expands the beam's numerical aperture. The microlens performs a beamsplitting operation, dividing the radiation primarily between a +1-order diffracted beam diverging approximately from point  $P_1$  and a zero-order undiffracted beam diverging from point  $P_0$ . A small portion of the transmitted radiation goes into other diffraction orders (e.g., the

illustrated -1 and -2 orders). Only the +1 transmitted order is used; all other orders are excluded by apertures or axial order-blocking masks either before or after reflection from the workpiece. (0-order, -1-order, and -2-order blocking masks are illustrated in Figures 6 and 7.)

The microlens is not configured to form a precise virtual image point at  $P_1$  in the +1 order; instead it shapes the beam wavefront so that it converges to a precise geometric image point on the workpiece, with zero aberration, after traversing the projection optics. Any projection system aberrations are nullified by the microlens.

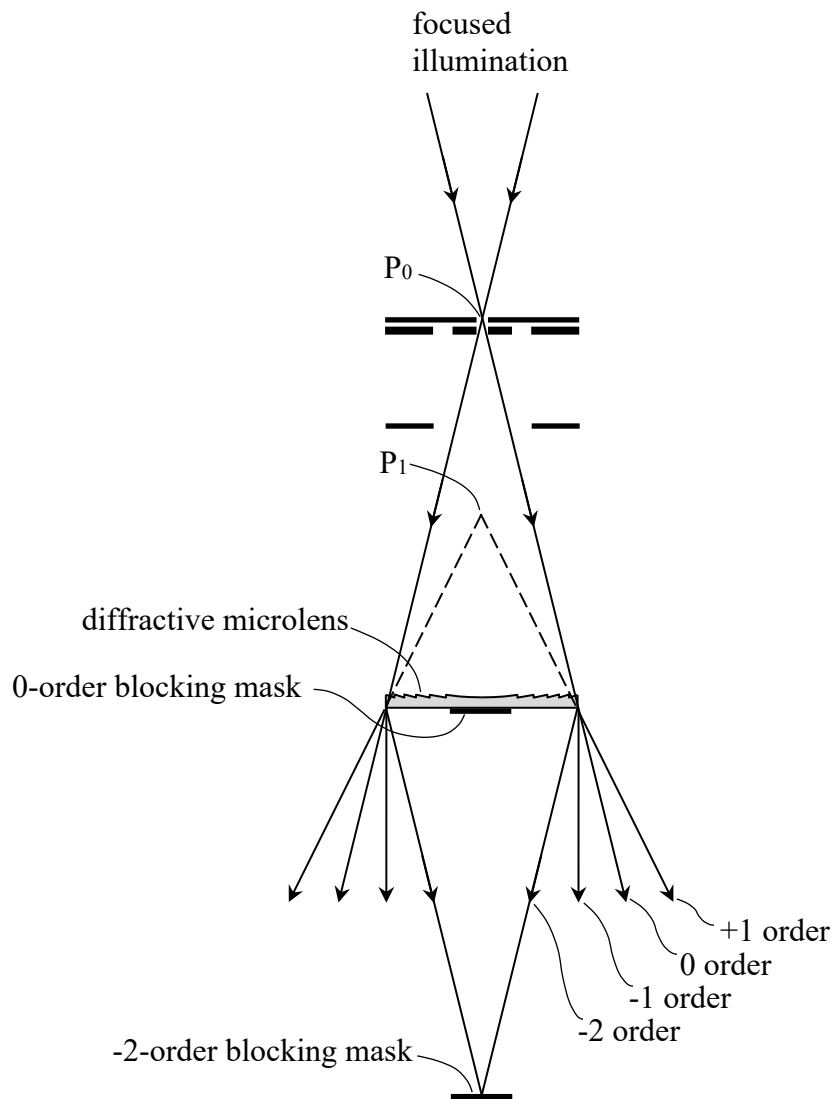


Figure 7

The reflected light path through the sensor unit is illustrated in Figure 8. The reflected zero order is blocked by the axial mask on the microlens, and the microlens divides the reflected +1 order into two beams, a diffracted beam directed back toward the source point  $P_0$ , and an

undiffracted beam, which passes through point  $P_1$  and illuminates an annular zone surrounding the source. (Other diffraction orders are excluded, e.g. by the annular mask in Figure 8.) The diffracted beam partially intercepts a small, annular focus detector centered at  $P_0$ , which provides a confocal signal for focus control. The undiffracted beam intercepts a larger, annular far-field detector, which is subdivided into four quadrant cells of a position-sensing detector for step-height measurement. The detector elements are illustrated in Figure 9.

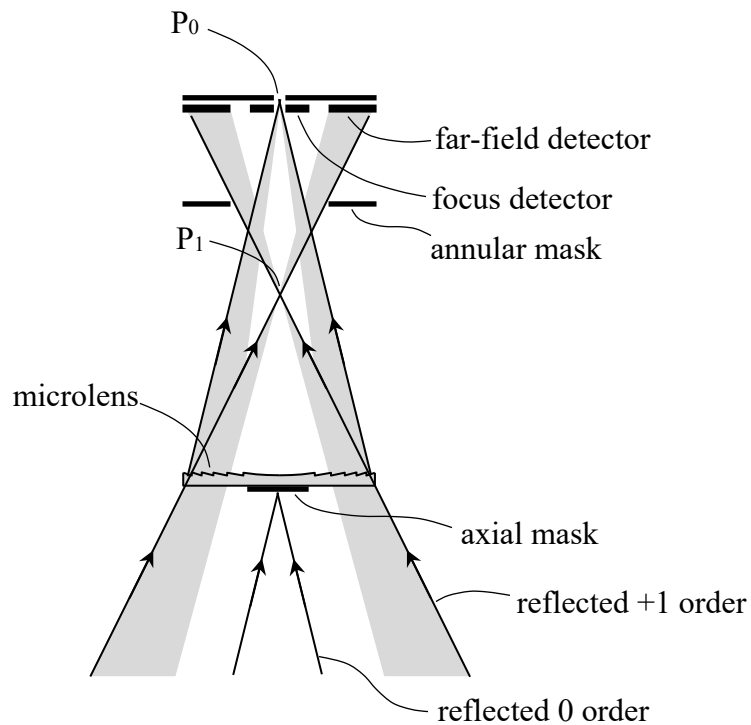


Figure 8

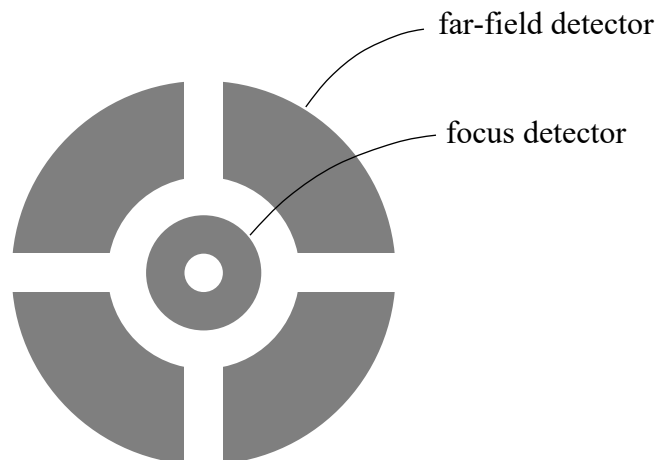


Figure 9

The beamsplitting microlens structure is illustrated in cross-section in Figure 10. The lens is similar to a phase-Fresnel lens [10], which is blazed for maximum efficiency in the first order, except that the blaze angle is reduced by a factor of two. Such a lens will direct approximately 40% of the transmitted radiation into the first order, 40% into the zero order, and the remainder into other extraneous orders. The annular lens zones are approximately circular, but are somewhat distorted compensate for off-axis aberrations in the projection system.



Figure 10

An alternative microlens structure is illustrated in Figure 11. In this design the lens power is divided between a meniscus refractive element and a phase zone-plate lens, a type of diffractive lens that has a rectangular zone profile (not the sawtooth profile of a phase Fresnel lens). The profile depth is determined to extinguish the zero diffraction order, and the transmitted energy is mostly divided between the +1 and -1 orders (approximately 40% each). In this case the two lens-transmitted beams on the return path in Figure 8 are both diffracted; the undiffracted order is extinguished. The diffractive structure of this lens may be more easily manufacturable than a phase-Fresnel lens (although it would generate more extraneous diffraction orders, which could be problematic for stray light control). The meniscus refractive surface can be spherical; its aberrations would be fully corrected by the diffractive surface.

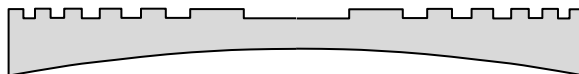


Figure 11

A limitation of the above-described sensor unit is that the confocal signal is not sensitive to the sign of the focus error. Two confocal sensors with slightly different focus offsets (one positive, one negative) can be combined to provide an accurate, signed focus signal. The sensor unit can be modified, as illustrated in Figures 12A-C, to do this. A glass plate has a backside mirror coating with a small transparent aperture at point  $P_0$  through which the illumination beam transmits. An annular focus detector is formed on the opposite side of the plate with an inner aperture just large enough to transmit the beam. A double-sided detector is used, which has separate sensor elements for detecting radiation coming from above or below the detector. (The upward- and downward-sensing elements can be overlaid, or can be formed on separate azimuthal zones of the annular detector.) When the microscope is in focus the reflected radiation is focused back to point  $P_0$  and the detector only senses a small signal from the beam's diffraction tails (Figure 12A). As the return focus point moves away from the illumination

source (Figure 12B), the annular detector becomes underfilled on the front side and overfilled on the back side, resulting in a higher signal from the back. As the focus moves toward the source (Figure 12C) the front side becomes overfilled and the back side underfilled, so the signal balance shifts toward the front. The difference between the front and back signals provides an accurate, signed measure of the focus offset.

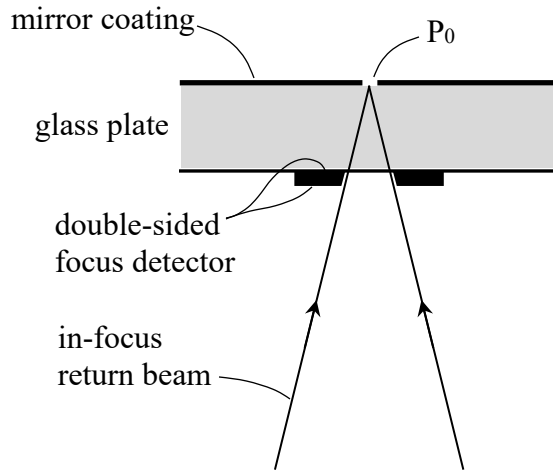


Figure 12A

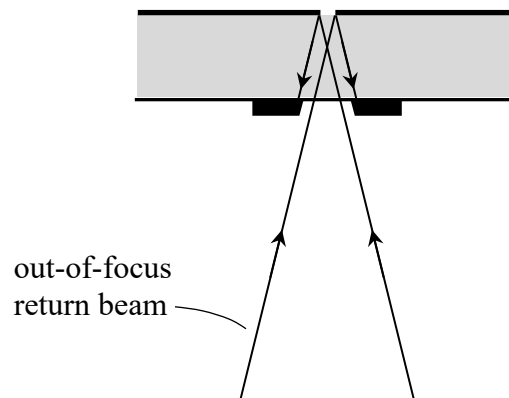


Figure 12B

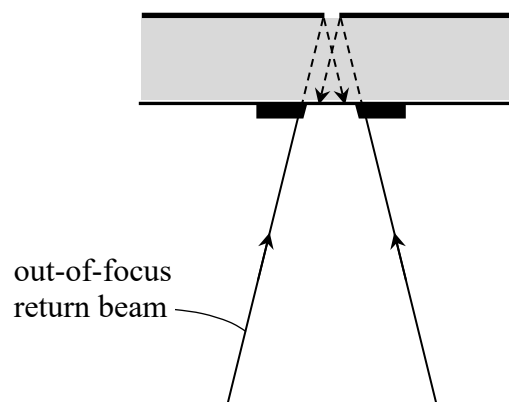


Figure 12C

## References

- [1] Precitech (a division of AMETEK, Inc.), <https://www.precitech.com/Nanoform<sup>®</sup>L1000>,  
<https://www.precitech.com/product/largeframelathesoverview/nanoforml1000>
- [2] John E. Bjorkholm, “EUV Lithography—The Successor to Optical Lithography?”, Intel Technology Journal Q3’98. <https://smtnet.com/library/files/upload/EUV-Lithography2.pdf>
- [3] Dmitriy L. Voronov et al., “High-efficiency 5000 lines/mm multilayer-coated blazed grating for extreme ultraviolet wavelengths”, *Optics Letters* 35, 2615-2617 (2010).  
<https://doi.org/10.1364/OL.35.002615>
- [4] F. Siewert et al., “Gratings for synchrotron and FEL beamlines: a project for the manufacture of ultra-precise gratings at Helmholtz Zentrum Berlin”, *J. Synchrotron Rad.* 25, 91–99 (2018).  
<https://journals.iucr.org/s/issues/2018/01/00/x15026/x15026.pdf>
- [5] K. Johnson, “EUV Source Optics with 100% OOB Exclusion”, 2018 EUVL Workshop (P14), <https://euvlitho.com/>
- [6] Stone, Thomas, and Nicholas George. "Hybrid diffractive-refractive lenses and achromats." *Applied Optics* 27, no. 14 (1988): 2960-2971.
- [7] Wood, Andrew P. "Hybrid refractive-diffractive lens for manufacture by diamond turning." In *Commercial Applications of Precision Manufacturing at the Sub-Micron Level*, vol. 1573, pp. 122-129. International Society for Optics and Photonics, 1992.
- [8] Languy, Fabian, Cédric Lenaerts, Jérôme Loicq, and Serge Habraken. "Achromatization of solar concentrator thanks to diffractive optics." (2009).
- [9] Rostalski, Hans-Juergen, Alexander Epple, and Heiko Feldmann. "Use of diffractive lenses in lithographic projection lenses." In *International Optical Design Conference*, p. WD4. Optical Society of America, 2006.
- [10] Miyamoto, K., 1961. The phase Fresnel lens. *JOSA*, 51(1), pp.17-20.